Dark Matter, Supersymmetry, and the Early Discovery Potential at the LHC

SUSY2010, Bonn, Germany
August 23-29, 2010

[PN]
Northeastern University, Boston, MA, USA

Outline

- Tensions in SUSY vs dark matter experiments
  WMAP, PAMELA, EGRET, FERMI–LAT, CDMSII, XENON100, COGENT, DAMA-LIBRA, $\cdots$
- Resolution needs extensions of the standard dark matter as $\tilde{\chi}$. To resolve tensions consider two proposals
  - $U(1)^n$ hidden sector extension of SUGRA models
  - Multicomponent visible sector + hidden sector dark matter in SUGRA models
- Dark matter - LHC connection
- Early SUSY discovery at the LHC at $\sqrt{s} = 7$ TeV with 1fb^{-1} of data.

Dark matter experiments

1. WMAP CDM relic density: $\boldsymbol{\Omega_{CDM} h^2 \simeq .1}$.
2. Positron flux (PAMELA)
3. Anti-proton flux (PAMELA, CAPRICE, BESS)
4. Photon flux (EGRET, FERMI-LAT)
5. CDMS II and XENON100 limits
6. COGENT: Excess in the DAMA-LIBRA sensitive region

There are significant tensions among these results if one wants to understand them within a single theoretical scheme.

Pamela Positron Excess

Difficult to explain Pamela results in the conventional SUSY models. However, there are many possibilities to explain Pamela.

- Astrophysical origin: The signal could be of astrophysical origin such as from pulsars.
- Particle physics models: It is interesting to investigate particle physics models which could explain this phenomenon.
  - Pamela excess a signal from the hidden sector. Dark matter resides in the hidden sector but it can annihilate into the SM particles.
  - SUSY model with neutralino as dark matter but with an extended hidden sector.
  - Multicomponent SUSY dark matter consisting of Majorana and Dirac particles as dark matter.
  - Others $\cdots$

Positron Excess vs WMAP

The basic issue: one needs

$$< \sigma v >\sim 10^{-24}\mathrm{cm}^3/\mathrm{s} \quad \textbf{positron excess}$$
$$< \sigma v >\sim 10^{-26}\mathrm{cm}^3/\mathrm{s} \quad \textbf{relic density}$$

Various possibilities for resolution

- Breit -Wigner pole enhancement of $< \sigma v >$ in the galaxy
  Feldman, Liu, PN, Phys. Rev. D **79**, 063509 (2009) arXiv:0810.5762 .
- The boost from coannihilation B_{Co} of the neutralino in the visible sector with gauginos and higgsinos in the hidden sector to enhance the relic density.
  Feldman, Liu, PN, Nelson, Phys. Rev. D **80**, 075001 (2009), arXiv:0907.5392.
- Sommerfeld enhancement
- Non-thermal processes to enhance relic density.
- Others $\cdots$

Enhancement of annihilation cross section in the galaxy

Feldman, Liu, PN, PRD 79, 063509 (2009)

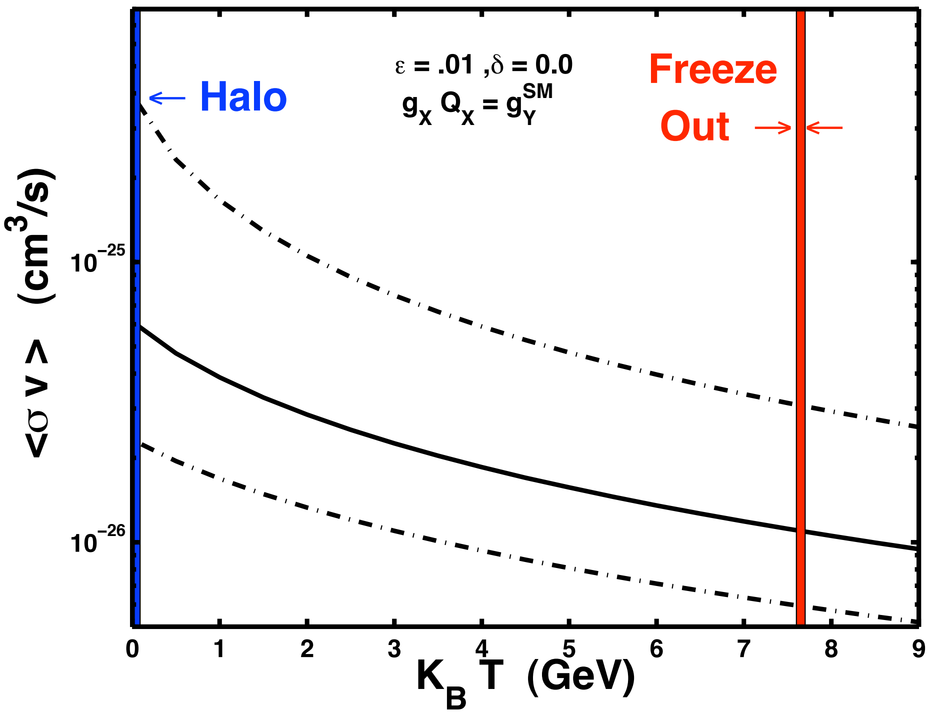

Explaining PAMELA excess in SUSY

Positron Flux from neutralino annihilation
Turner and Wilczek (1990)

$$\chi^0 + \chi^0 \to W^+W^-, \; W^+ \to e^+\nu$$

Need $<\sigma v>\sim 10^{-24}\mathrm{cm}^3/\mathrm{s}$ for positron excess but this underproduces the relic density by a factor of about 50-100 below the desired value since

$$\Omega h^2 \propto 1/\int <\sigma v> x^{-2}dx, \;\; x = m_{\chi^0}/T.$$

Need $<\sigma v>\sim 10^{-26}cm^3/s$ for relic density consistent with WMAP.

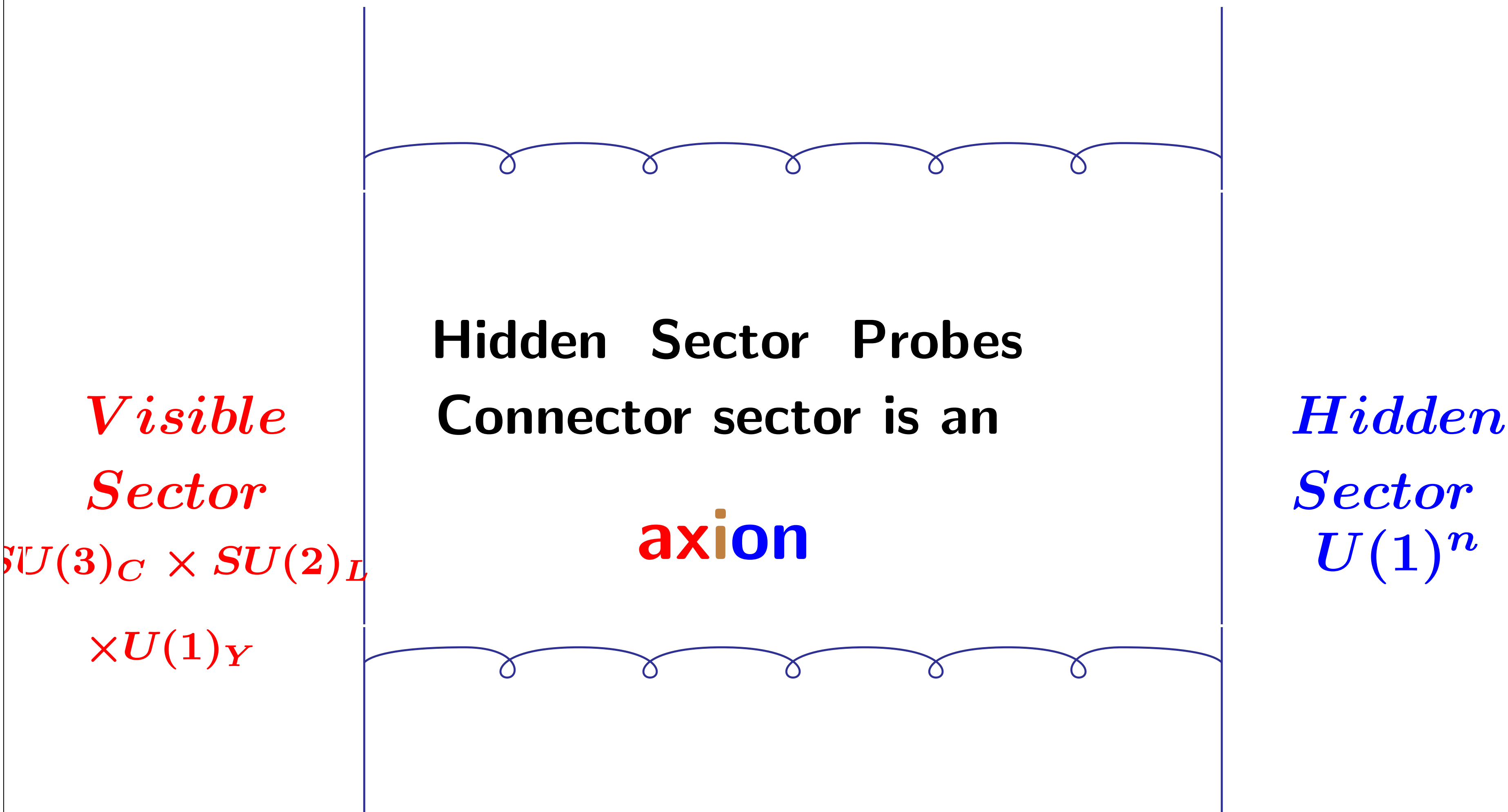

Stueckelberg mechanism: Kors, PN

Stueckelberg from couplings to 2-form tensor

$$L_0 = -\frac{1}{12} H^{\mu\nu\rho} H_{\mu\nu\rho} - \frac{1}{4} F^{\mu\nu} F_{\mu\nu} + \frac{m}{4} \epsilon^{\mu\nu\rho\sigma} F_{\mu\nu} B_{\rho\sigma}$$

$$F_{\mu\nu} = \partial_\mu A_\nu - \partial_\nu A_\mu, \;\; H_{\mu\nu\rho} = \partial_\mu B_{\nu\rho} + \partial_\nu B_{\rho\mu} + \partial_\rho B_{\mu\nu}.$$

We can write L in an alternative form

$$L_1 = -\frac{1}{12} H^{\mu\nu\rho} H_{\mu\nu\rho} - \frac{1}{4} F^{\mu\nu} F_{\mu\nu} - \frac{m}{6} \epsilon^{\mu\nu\rho\sigma} (H_{\mu\nu\rho} A_\sigma + \sigma \partial_\mu H_{\nu\rho\sigma})$$

We can recover L by integrating over σ which gives

$$d^* H = 0$$

and intserting it back in L_1 gives L. Instead suppose we solve for H

$$H^{\mu\nu\rho} = -m \epsilon^{\mu\nu\rho\sigma} (A_\sigma + \partial_\sigma \sigma)$$

Insertion back in L_1 gives

$$L_2 = -\frac{1}{4} F^{\mu\nu} F_{\mu\nu} - \frac{m^2}{2} (A_\sigma + \partial_\sigma \sigma)^2$$

Hidden sector: $U(1)$ Stueckelberg extension of the SM which communicates with the SM via a connector sector which is an axion which transforms dually under $U(1)_Y$ and $U(1)_X$. B. Kors, PN, PLB 586, 2004, **Feldman, Liu, PN (2006)**

$$L_{st} = -\frac{1}{2}(\partial_\mu + M_1 C_\mu + M_2 B_\mu)^2$$

Invariant under

$$\delta_Y B_\mu = \partial_\mu \lambda_Y\,,\ \delta_Y \sigma = -M_2 \lambda_Y$$
$$\delta_Y C_\mu = \partial_\mu \lambda_X\,,\ \delta_X \sigma = -M_1 \lambda_X$$

Vector boson mass matrix

$$\begin{pmatrix} M_1^2 & M_1 M_2 & 0 \\ M_1 M_2 & M_2^2 + \frac{1}{4} g_Y^2 v^2 & -\frac{1}{4} g_Y g_2 v^2 \\ 0 & -\frac{1}{4} g_Y g_2 v^2 & \frac{1}{4} g_2^2 v^2 \end{pmatrix}, \quad \epsilon = M_2/M_1$$

Constraints on Stueckelberg Z' boson from D0
1008.2023 [hep-ex], August 11, 2010

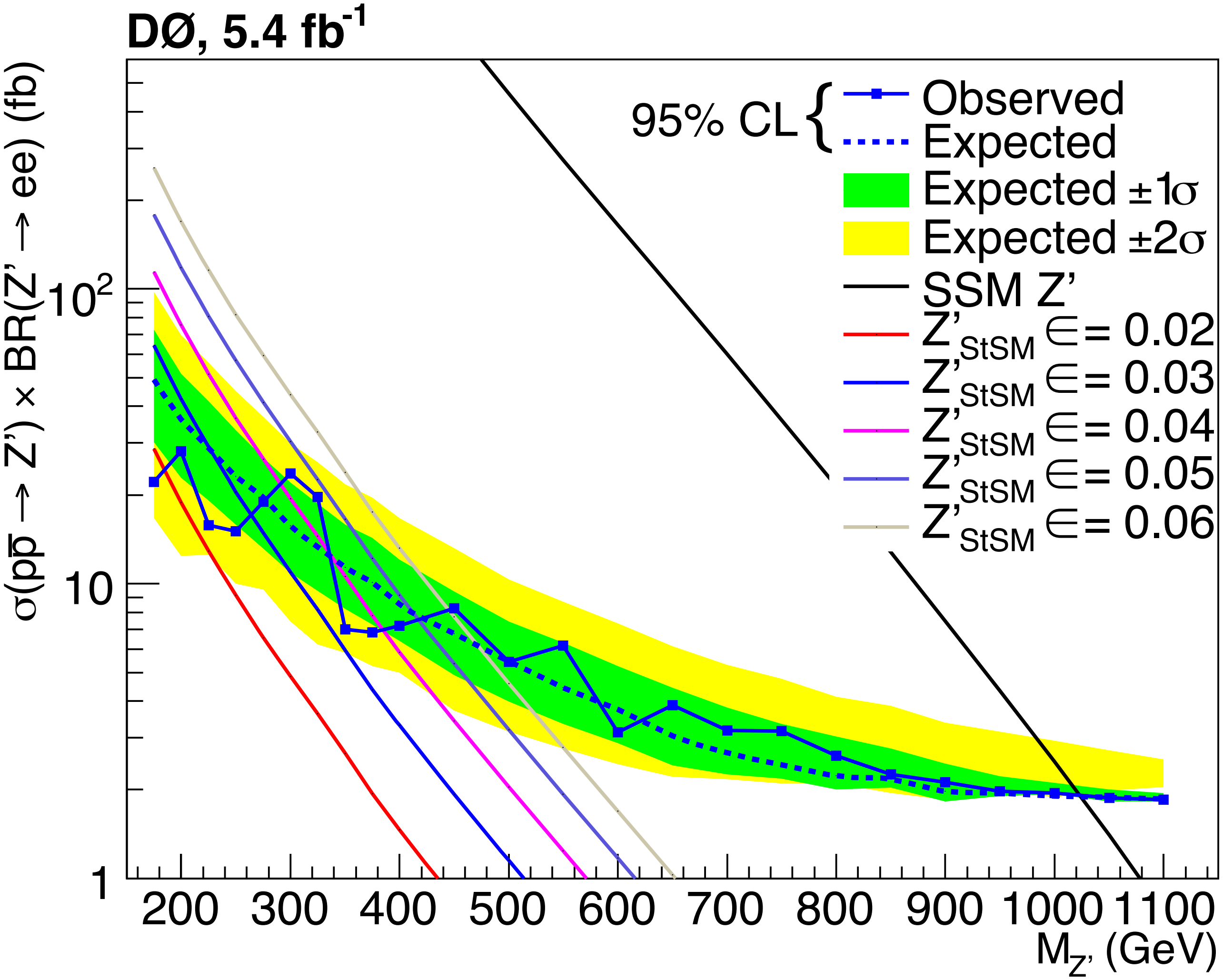

A Stueckelberg Z' if seen would most likely be an indicator of an underlying string physics

Feldman, Liu, PN

Stueckelberg Z prime

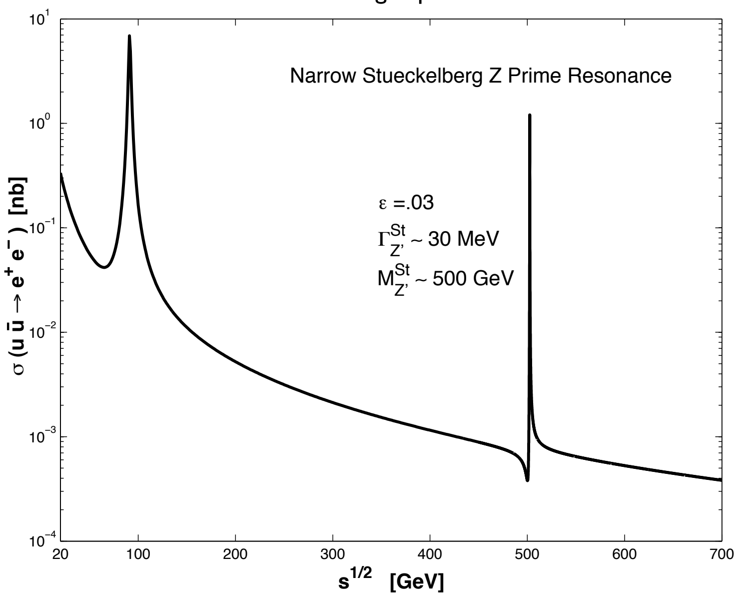

PN, yamada, Yamaguchi
Antoniadis, Binakli, Quiros

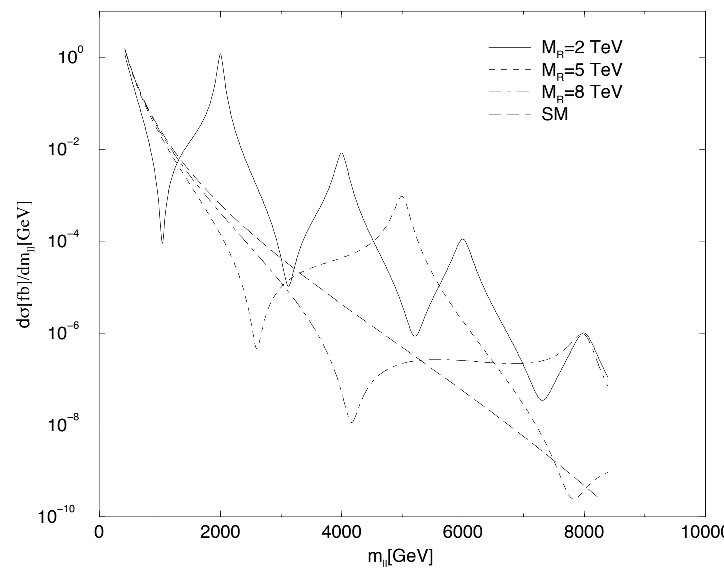

Fig. 2. Differential cross section $d\sigma/dm_{ll}$ as a function of the invariant mass m_{ll} of the charged lepton pair for three different values of the compactified dimension M_R. For comparison the analysis for the SM case is also shown.

The $U(1)^n$ extended SUGRA model

Kors, PN, JHEP 0412:005,2004

$$\mathcal{L} = \mathcal{L}_{\mathrm{MSSM}} + \mathcal{L}_{U(1)^n} + \Delta\mathcal{L}$$

$$\Delta\mathcal{L} = \int d^2\theta d^2\bar{\theta} \sum_{m=1}^{N_S} \left[\sum_{l=1}^{N_V} M_{l,m} V_l + (\Phi_m + \bar{\Phi}_m) \right]^2 ,$$

where $V = \{B, X, X', X'' \ldots\}$ are vector supermultiplets which include the hypercharge gauge multiplet B, and Φ_m are a collection of chiral supermultiplets and $(N_S, N_V > N_S)$ are the number of (axions,vectors). The neutralino sector is $(4 + 2n)$ dimensional.

$$\mathcal{M}^{[x]} = \left(\begin{array}{c|c} [\mathrm{M}_1]_{2n\times 2n} & [\mathrm{M}_2]_{2n\times 4} \\ \hline [\mathrm{M}_2]^T_{4\times 2n} & [\mathrm{M}_{\mathrm{MSSM}}]_{4\times 4} \end{array} \right)$$

The off diagonal terms are typically of size $\epsilon \equiv M_2/M_1 << 1$.
Tests in the EW region: Feldman, Liu, PN (2006)

Boost via Neutralino Coannihilations (B_{Co}) with a $U(1)^n$ hidden gauge sector in extended SUGRA

Feldman, Liu, PN, Nelson, PRD 80, 075001 (2009)

Neutralino coannihilations with the hidden sector produce an effective enhancement of the relic density by a factor B_{Co}

$$B_{Co} = \frac{(\Omega_\chi h^2)_{observed}}{(\Omega_\chi h^2)_{MSSM}} \simeq (1 + \frac{d_h}{d_v})^2$$

$d_h\,(d_v)$ are the number of degrees of freedom degenerate with the neutralino in the hidden (visible) sectors.

- Pure Wino Model (PWM): $m_\chi^\pm \sim m_{\chi^0}$, $d_v = 6$, $d_h = 2n{\times}2$

$$B_{Co} = (1 + \frac{2}{3}n)^2 = 9 \quad [\text{for } U(1)^3]$$

- Higgsino - Wino Model (PWM): $m_\chi^\pm$ and m_{χ^0} are split, $d_v = 2$, $d_h = 2n{\times}2$

$$B_{Co} = (1 + 2n)^2 = 49 \quad [\text{for } U(1)^3]$$

Monochromatic Sources

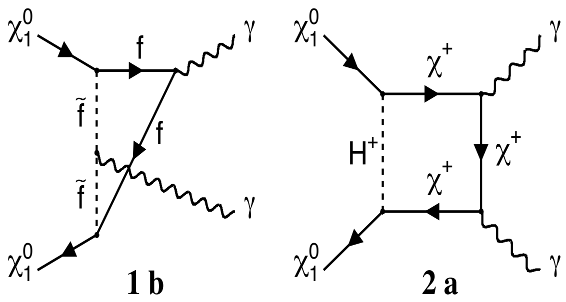

Figure: Neutralino annihilation into 2γ and similar diagrams for γZ. Bern etal; Bergstrom etal.

PWM produces stronger monochromatic sources than HWM and provides a distinguishing feature between the PWM and HWM.

Monochromatic sources from PWM

$$\mathbf{PWM}: \langle \sigma v \rangle^{1\ \mathrm{loop}}_{\gamma\gamma} = 2.0 \times 10^{-27}\ \mathrm{cm}^3/\mathrm{s}.$$

$$\mathbf{PWM}: \langle \sigma v \rangle^{1\ \mathrm{loop}}_{\gamma Z} = 1.3 \times 10^{-26}\ \mathrm{cm}^3/\mathrm{s}.$$

Monochromatic sources from HWM

$$\mathbf{HWM}: \langle \sigma v \rangle^{1\ \mathrm{loop}}_{\gamma\gamma} = 1.6 \times 10^{-28}\ \mathrm{cm}^3/\mathrm{s},$$

$$\mathbf{HWM}: \langle \sigma v \rangle^{1\ \mathrm{loop}}_{\gamma Z} = 1.0 \times 10^{-27}\ \mathrm{cm}^3/\mathrm{s},$$

FERMI-LAT results on $\gamma\gamma$ and γZ

E_γ (GeV)	95%CLUL (10^{-9} cm^{-2}s^{-1})	$\langle\sigma v\rangle_{\gamma\gamma}$ [γZ] (10^{-27} cm^{3}s^{-1}) NFW	Einasto	Isothermal	$\tau_{\gamma\gamma}$ [γZ] (1 NFW	Einasto
30	3.5	0.3 [2.6]	0.2 [1.9]	0.5 [4.5]	17.6 [4.2]	17.8 [4.2
40	4.5	0.7 [4.2]	0.5 [3.0]	1.2 [7.2]	10.1 [2.9]	10.3 [2.9
50	2.4	0.6 [2.7]	0.4 [1.9]	1.0 [4.6]	15.5 [5.0]	15.7 [5.1
60	3.1	1.1 [4.2]	0.8 [3.0]	1.8 [7.3]	9.8 [3.5]	10.0 [3.5
70	1.2	0.6 [2.0]	0.4 [1.4]	1.0 [3.4]	21.6 [8.2]	21.9 [8.3
80	0.9	0.5 [1.7]	0.4 [1.2]	0.9 [2.9]	26.0 [10.4]	26.4 [10.
90	2.6	2.0 [6.0]	1.5 [4.3]	3.5 [10.3]	7.7 [3.2]	7.8 [3.2]
100	1.4	1.4 [3.8]	1.0 [2.8]	2.4 [6.6]	12.6 [5.4]	12.8 [5.4
110	0.9	1.0 [2.7]	0.7 [1.9]	1.7 [4.6]	18.9 [8.2]	19.2 [8.3
120	1.1	1.6 [4.0]	1.1 [2.9]	2.7 [6.9]	13.3 [5.9]	13.5 [6.0
130	1.8	3.0 [7.3]	2.1 [5.3]	5.1 [12.6]	7.6 [3.4]	7.8 [3.5]
140	1.9	3.5 [8.4]	2.5 [6.0]	6.0 [14.3]	7.0 [3.2]	7.1 [3.3]
150	1.6	3.5 [8.2]	2.5 [5.9]	6.0 [14.1]	7.5 [3.5]	7.6 [3.5]
160	1.1	2.7 [6.3]	2.0 [4.5]	4.7 [10.9]	10.2 [4.8]	10.4 [4.8
170	0.6	1.7 [4.0]	1.3 [2.9]	3.0 [6.8]	17.0 [8.0]	17.2 [8.1
180	0.9	2.7 [6.1]	1.9 [4.4]	4.6 [10.4]	11.6 [5.5]	11.8 [5.6
190	0.9	3.2 [7.1]	2.3 [5.1]	5.5 [12.2]	10.4 [4.9]	10.5 [5.0
200	0.9	3.3 [7.3]	2.4 [5.2]	5.7 [12.5]	10.6 [5.1]	10.8 [5.1

Flux, annihilation cross-section upper limits, and decay lifetime lower limits:

Abdo et.al., PRL 104, 091302 (2010), arXiv:1001.4836[Astro–ph.HE].

HWM: (.16, 1.0) safe

PWM: (2, 13) near the edge .

Dark Matter - LHC Connection

Gaugino -Higgsino Content of the Neutralino and LHC Signatures

The signatures at the LHC will be dependent on the gaugino vs higgsino content of the neutralino. Thus the neutralino wave function can be expanded as

$$\chi = \alpha\tilde{\lambda}_B + \beta\tilde{\lambda}_W + \gamma\tilde{h}_1 + \delta\tilde{h}_2$$

For illustration we consider two models.

- Model 1: As the first example we consider the mixed Higgino-Wino model (HWM) which has a substantial higgsino component.
- Model 2: As the second example we consider the pure Wino model (PWM) where the neutralino is almost 100% wino. Models of this type arise in anomaly mediated breaking. One characteristic of such models is that the lighter chargino and the neutralino are essentially degenerate $m_{\chi_1^\pm} \simeq m_{\chi^0}$.

These models lead to distinguishable signatures at the LHC.

Effective mass distribution

Feldman, Liu, PN, Nelson, PRD D 80, 075001 (2009)

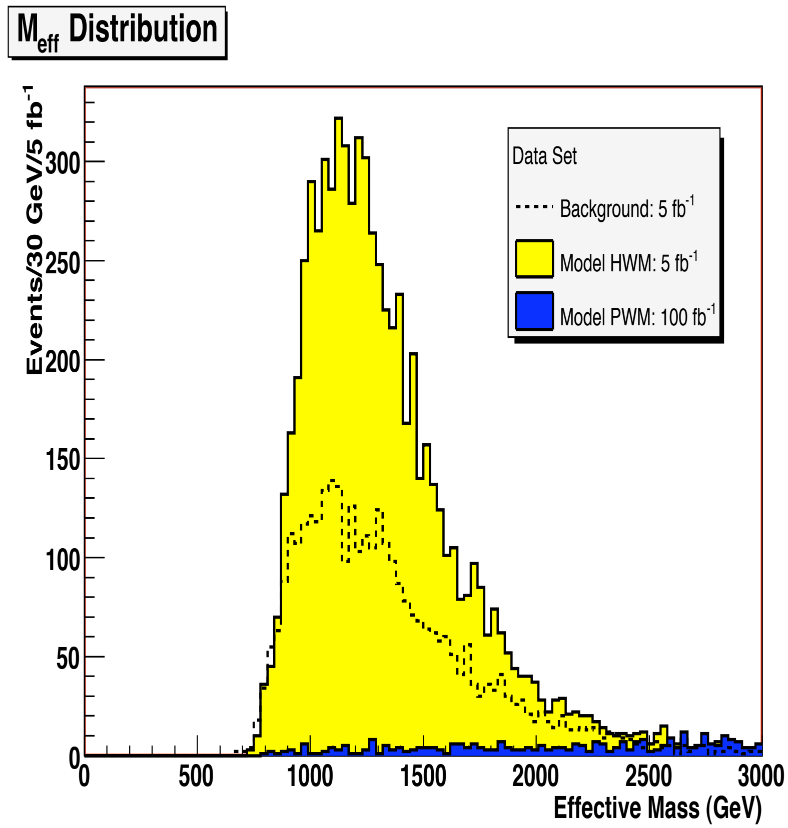

M_{eff} is defined as the scalar sum of the transverse momenta of four hardest jets $P_T \geq (200, 150, 50, 50)$ GeV in the event plus missing energy ($E_T^{miss} \geq 200$ GeV).The plot is of events for the Higgsino-Wino model (for 5fb^{-1} yellow) and for Pure Wino model (100 fb^{-1} blue).

Hints for SUSY

- LEP data on gauge couplings: unification with low lying sparticles can be achieved.
- A significant deviation of $(a_\mu^{exp} - a_\mu^{SM})$ for the muon anomalous magnetic moment.

  Recent analyses hint at a deviation between $(3-4)\sigma$ away from the standard model prediction and the largest discrepany claimed is

  $$a_\mu^{exp} - a_\mu^{SM} = +31.6(7.9) \times 10^{-10}$$

  T. Teubner, K. Hagiwara, R. Liao, A. D. Martin and D. Nomura, arXiv:1001.5401 [hep-ph]

  M. Passera, W. J. Marciano and A. Sirlin, arXiv:1001.4528 [hep-ph].

  A significant correction points to low lying sparticles in SUSY

  T. C. Yuan, R. L. Arnowitt, A. H. Chamseddine and P.N., Z. Phys. C **26**, 407 (1984); D. A. Kosower, L. M. Krauss and N. Sakai, Phys. Lett. B **133**, 305 (1983).
- A hint of deviation from the SM value of $BR(b \longrightarrow s\gamma)$.

The Hint from $b \longrightarrow s\gamma$

Chen, Feldman, Liu, PN: Phys. Lett. B **685**, 174 (2010), arXiv:0911.0217

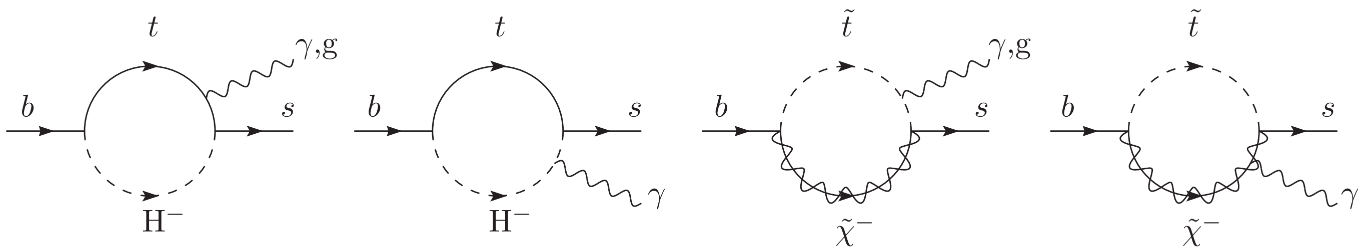

- The experimental value of $b \longrightarrow s\gamma$ given by the Heavy Flavor Averaging Group (HFAG) along with BABAR, Belle, and CLEO experiments give

$$BR(b \longrightarrow s\gamma) = (3.52 \pm .23 \pm .09) \times 10^{-4}$$

- The SM value including NNLO corrections is

$$B(b \longrightarrow s\gamma) = (3.15 \pm .23) \times 10^{-4}$$

  The SM value lies lower than the HFAG value. The result implies a low lying charged Higgs which gives a positive contribution (JoAnn Hewett (1993)).

- If there is a significant cancellation between the charged Higgs and the chargino loops, then the chargino and stop must also be relatively light and thus a good chance of seeing one or more of the sparticles in the early runs at the LHC.

Early SUSY Discovery

Baer, Barger, Lessa, Tata, JHEP 1006, 102 (2010)

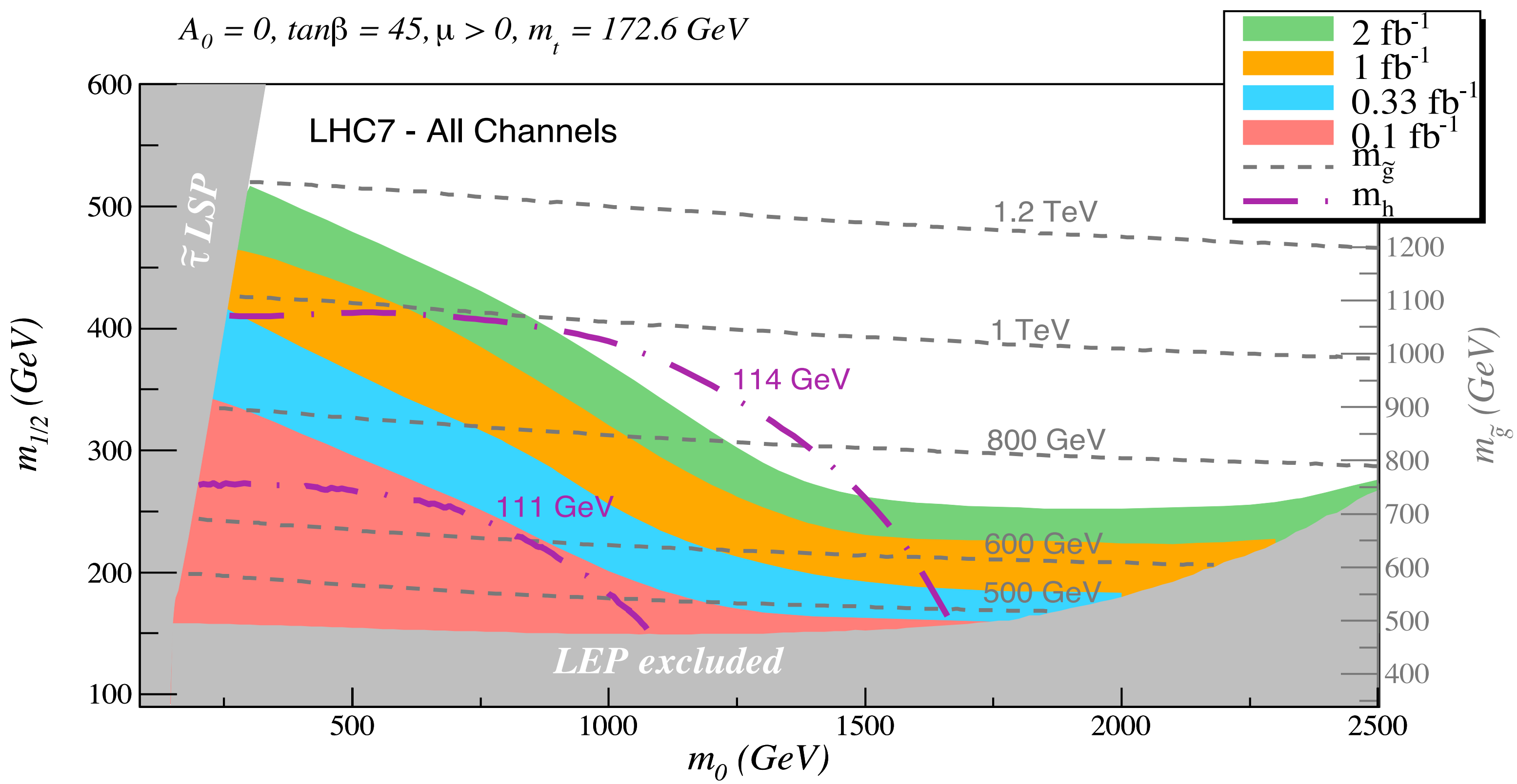

C. W. Bauer, Z. Ligeti, M. Schmaltz, J. Thaler and D. G. E. Walker,
H K. Dreiner, M Kramer, J M. Lindert, B O'Leary,
H. Baer, V. Barger, A. Lessa and X. Tata,
N. Bhattacharyya, A. Datta and S. Poddar,
D. S. M. Alves, E. Izaguirre and J. G. Wacker,
K. Desch, H. K. Dreiner, S. Fleischmann, S. Grab, P. Wienemann.

Altunkaynak, Holmes, PN, Nelson, Peim
arXiv: 1008.3423 [hep-ph]

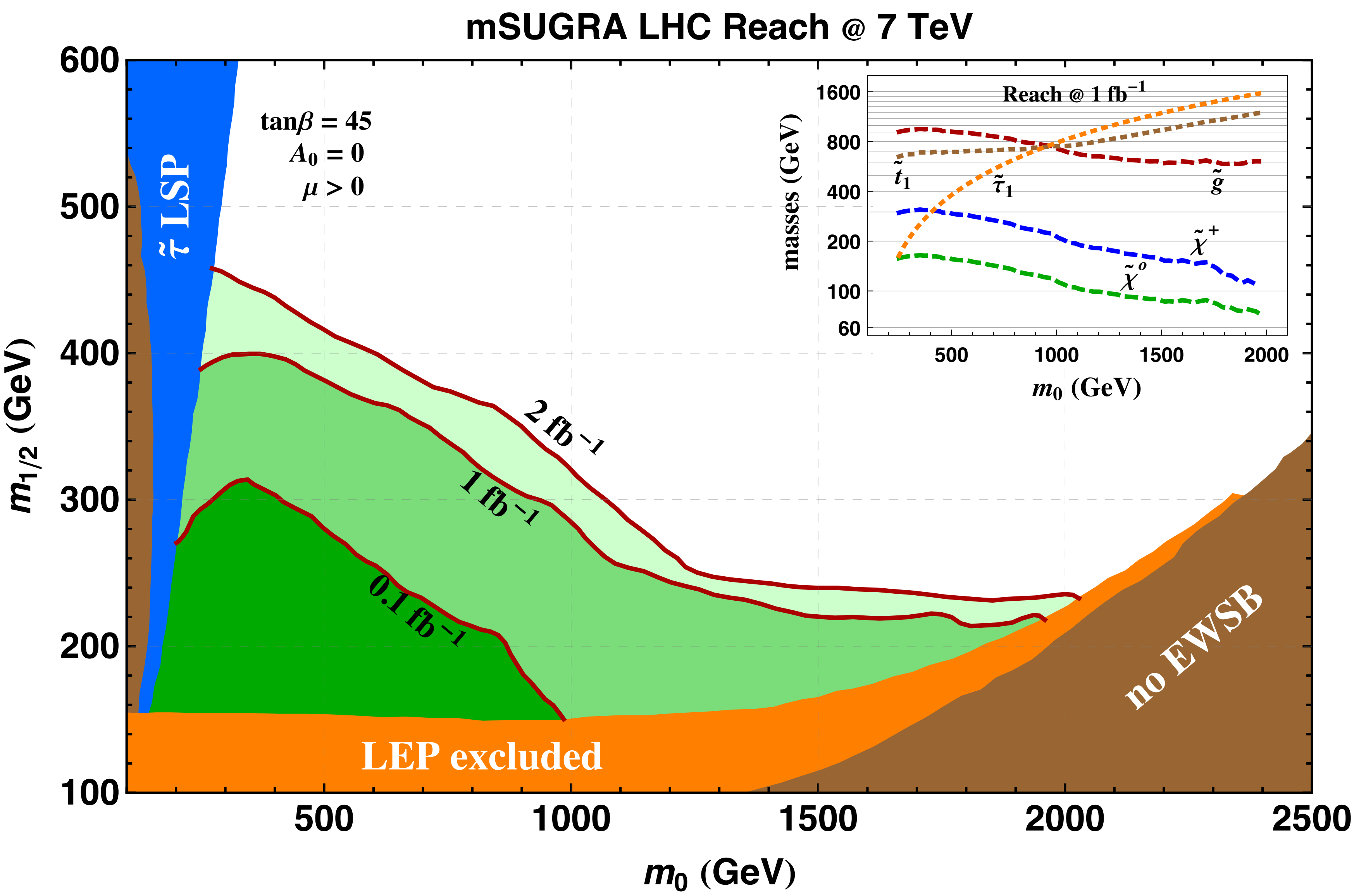

Altunkaynak, Holmes, PN, Nelson, Peim
arXiv: 1008.3423 [hep-ph]

VII. TABLES

A Display of Signatures/Cuts Used in Early Discovery Analysis at the LHC at $\sqrt{s} = 7$ TeV

	Signature Name	Description of Cut	
1	MET only	$n(\ell) = 0$	$p_T\,(j_1) < 20$ GeV
2	mono-jets	$n(\ell) = 0$	$p_T(j_1) \geq 100$ GeV, $p_T(j_2) < 20$ GeV
3	multi-jets200	$n(\ell) = 0$	$p_T(j_1) \geq 200$ GeV, $p_T(j_2) \geq 150$ GeV, $p_T(j_4) \geq 50$ GeV
4	multi-jets100	$n(\ell) = 0$	$p_T(j_1) \geq 100$ GeV, $p_T(j_2) \geq 80$ GeV, $p_T(j_4) \geq 40$ GeV
5	hard-jets500	$n(\ell) = 0$	$p_T(j_2) \geq 500$ GeV
6	hard-jets350	$n(\ell) = 0$	$p_T(j_2) \geq 350$ GeV
7	multi-bjets1	$n(\ell) = 0$, $n(b) \geq 1$	
8	multi-bjets2	$n(\ell) = 0$, $n(b) \geq 2$	
9	multi-bjets3	$n(\ell) = 0$, $n(b) \geq 3$	
10	H_T500	$n(\ell) + n(j) \geq 4$	$p_T(1) \geq 100$ GeV , $\sum_{i=1}^{4} p_T(i) + \not{E}_T \geq 500$ GeV
11	H_T400	$n(\ell) + n(j) \geq 4$	$p_T(1) \geq 100$ GeV , $\sum_{i=1}^{4} p_T(i) + \not{E}_T \geq 400$ GeV
12	1-lepton100	$n(\ell) = 1$	$p_T(\ell_1) \geq 20$ GeV, $p_T(j_1) \geq 100$ GeV, $p_T(j_2) \geq 50$ GeV
13	1-lepton40	$n(\ell) = 1$	$p_T(l_1) \geq 20$ GeV, $p_T(j_2) \geq 40$ GeV
14	OS-dileptons100	$n(\ell^+) = n(\ell^-) = 1$	$p_T(\ell_2) \geq 20$ GeV, $p_T(j_1) \geq 100$ GeV, $p_T(j_2) \geq 50$ GeV
15	OS-dileptons40	$n(\ell^+) = n(\ell^-) = 1$	$p_T(\ell_2) \geq 20$ GeV, $p_T(j_2) \geq 40$ GeV
16	SS-dileptons100	$n(\ell^+ \mid \ell^-) = n(\ell) = 2$	$p_T(\ell_2) \geq 20$ GeV, $p_T(j_1) \geq 100$ GeV, $p_T(j_2) \geq 50$ GeV
17	SS-dileptons40	$n(\ell^+ \mid \ell^-) = n(\ell) = 2$	$p_T(\ell_2) \geq 20$ GeV, $p_T(j_2) \geq 40$ GeV
18	3-leptons100	$n(\ell) = 3$	$p_T(l_3) \geq 20$ GeV, $p_T(j_1) \geq 100$ GeV, $p_T(j_2) \geq 50$ GeV
19	3-leptons40	$n(\ell) = 3$	$p_T(l_3) \geq 20$ GeV, $p_T(j_2) \geq 40$ GeV
20	4^+-leptons	$n(\ell) \geq 4$	$p_T(l_4) \geq 20$ GeV, $p_T(j_2) \geq 40$ GeV
21	1-tau100	$n(\tau) = 1$	$p_T(\tau_1) \geq 20$ GeV, $p_T(j_1) \geq 100$ GeV, $p_T(j_2) \geq 50$ GeV
22	1-tau40	$n(\tau) = 1$	$p_T(\tau_1) \geq 20$ GeV, $p_T(j_2) \geq 40$ GeV
23	OS-ditaus100	$n(\tau^+) = n(\tau^-) = 1$	$p_T(\tau_2) \geq 20$ GeV, $p_T(j_1) \geq 100$ GeV, $p_T(j_2) \geq 50$ GeV
24	OS-ditaus40	$n(\tau^+) = n(\tau^-) = 1$	$p_T(\tau_2) \geq 20$ GeV, $p_T(j_2) \geq 40$ GeV
25	SS-ditaus100	$n(\tau^+ \mid \tau^-) = n(\tau) = 2$	$p_T(\tau_2) \geq 20$ GeV, $p_T(j_1) \geq 100$ GeV, $p_T(j_2) \geq 50$ GeV
26	SS-ditaus40	$n(\tau^+ \mid \tau^-) = n(\tau) = 2$	$p_T(\tau_2) \geq 20$ GeV, $p_T(j_2) \geq 40$ GeV
27	3^+-taus100	$n(\tau) \geq 3$	$p_T(\tau_3) \geq 20$ GeV, $p_T(j_1) \geq 100$ GeV, $p_T(j_2) \geq 50$ GeV
28	3^+-taus40	$n(\tau) \geq 3$	$p_T(\tau_4) \geq 20$ GeV, $p_T(j_2) \geq 40$ GeV
29	1^+-photon	$n(\gamma) \geq 1$	$p_T(j_2) \geq 40$ GeV

TABLE II: List of signatures and cuts used in the early discovery analysis. Our notation is as follows: $\ell = e, \mu$, $n(x)$ is the number of object x in the event, and $p_T(x_n)$ is the transverse momentum of the n^{th} hardest object x. We required $\not{E}_T \geq 200$ GeV and a minimum transverse sphericity of 0.2. The symbol | should be read as the logic "or," i.e. the cut $n\left(\tau^+ \mid \tau^-\right) = 2$ would be read "the number of τ^+ equals 2 or the number of τ^- equals 2."

$$\boldsymbol{H_T = \sum_{j=1}^{4} p_{Tj} + E_T^{miss}}$$

Altunkaynak, Holmes, PN, Nelson, Peim
arXiv: 1008.3423 [hep-ph]

Benchmarks for Early Discovery at $\sqrt{s} = 7$ TeV with 2 fb^{-1}

Label	NLSP	m_0	$m_{\frac{1}{2}}$	A_0	$\tan\beta$	δ_2	δ_3	$\sigma_{\rm SUSY}$ (pb)	$\sigma_{\rm SI}$ $(10^{-44}{\rm cm}^2)$
C1	$\chi_1^\pm$	1663	309	1508	32.9	0.553	-0.687	24.3	7.0
C2	$\chi_1^\pm$	449	330	176	20.3	-0.382	-0.151	2.4	3.7
C3	$\chi_1^\pm$	1461	361	1327	30.3	-0.241	-0.702	14.8	4.5
C4	$\chi_1^\pm$	1264	445	1775	24.7	0.718	-0.736	11.3	4.7
C5	$\chi_1^\pm$	240	313	-522	5.48	-0.376	-0.106	3.5	0.68
G1	$\widetilde{g}$	1694	755	-2128	45.7	0.745	-0.803	2.2	4.9
G2	$\widetilde{g}$	2231	639	2710	18.0	0.543	-0.850	24.2	3.0
G3	$\widetilde{g}$	2276	615	-2407	47.2	0.631	-0.784	3.1	2.6
G4	$\widetilde{g}$	2180	651	-2271	47.1	0.680	-0.817	5.8	8.3
G5	$\widetilde{g}$	2126	683	2924	38.0	0.580	-0.849	19.4	4.8
G6	$\widetilde{g}$	1983	749	-2332	46.3	0.562	-0.824	3.7	2.7
H1	A^o	2225	674	-2531	47.3	0.783	-0.703	0.3	0.92
S1	$\widetilde{\tau}_1$	117	394	0	15.9	-0.327	-0.177	1.4	1.4
S2	$\widetilde{\tau}_1$	101	446	-153	6.1	0.607	-0.207	0.4	0.48
S3	$\widetilde{\tau}_1$	102	470	183	15.3	0.603	-0.266	0.5	3.0
S4	$\widetilde{\tau}_1$	309	581	-613	27.7	0.839	-0.400	0.6	1.6
S5	$\widetilde{\tau}_1$	135	688	-184	5.7	-0.052	-0.499	0.4	1.6
S6	$\widetilde{\tau}_1$	114	404	27	13.0	-0.369	-0.267	2.0	3.0
S7	$\widetilde{\tau}_1$	114	518	87	10.4	0.266	-0.247	0.2	0.60
T1	$\widetilde{t}_1$	1726	548	4197	21.2	0.132	-0.645	2.3	5.0×10^{-3}
T2	$\widetilde{t}_1$	1590	755	3477	23.4	0.805	-0.803	3.8	9.4×10^{-2}

TABLE III: Benchmarks for *models discoverable* at the LHC at $\sqrt{s} = 7$ TeV with 2 fb^{-1} of integrated luminosity. The model inputs are given at $M_{GUT} = 2 \times 10^{16}$ GeV, sign$(\mu) = +1$, and $\delta_1 = 0$. The displayed masses are in GeV. All models satisfy REWSB and the experimental constraints as discussed in Sec. (II). The spin independent direct detection cross section, $\sigma_{\rm SI}$, is exhibited as well as the cross section $\sigma_{\rm SUSY}$ for the production of supersymmetric particles at $\sqrt{s} = 7$ TeV. Our analysis shows that all the models listed in this table are discoverable at the 5σ level above the background in *several channels* as exhibited in Fig. (5).

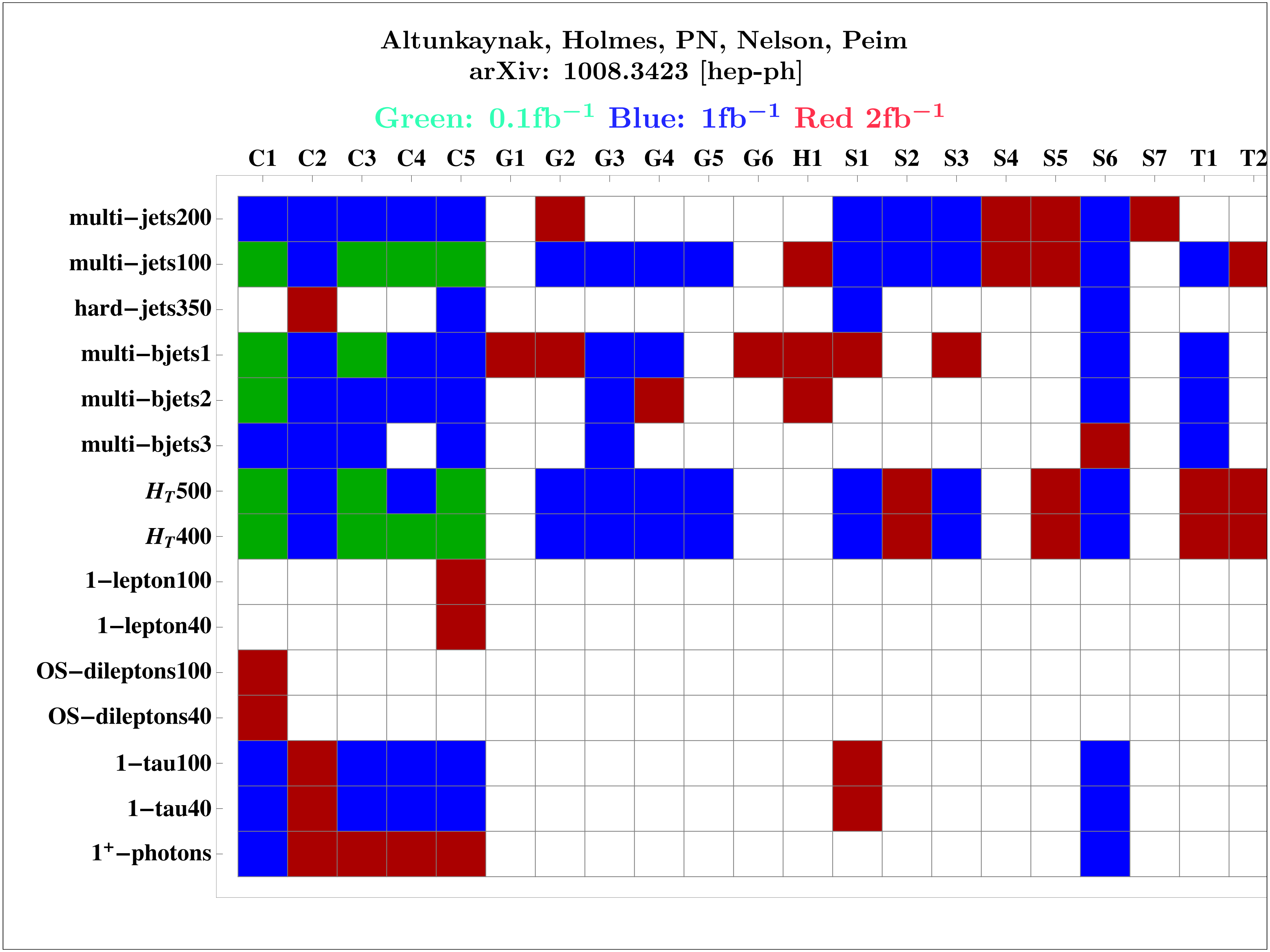

Altunkaynak, Holmes, PN, Nelson, Peim
arXiv: 1008.3423 [hep-ph]
Green: 0.1fb^{-1} Blue: 1fb^{-1} Red 2fb^{-1}
C1 C2 C3 C4 C5 G1 G2 G3 G4 G5 G6 H1 S1 S2 S3 S4 S5 S6 S7 T1 T2
multi−jets200
multi−jets100
hard−jets350
multi−bjets1
multi−bjets2
multi−bjets3
H_T500
H_T400
1−lepton100
1−lepton40
OS−dileptons100
OS−dileptons40
1−tau100
1−tau40
1$^+$−photons

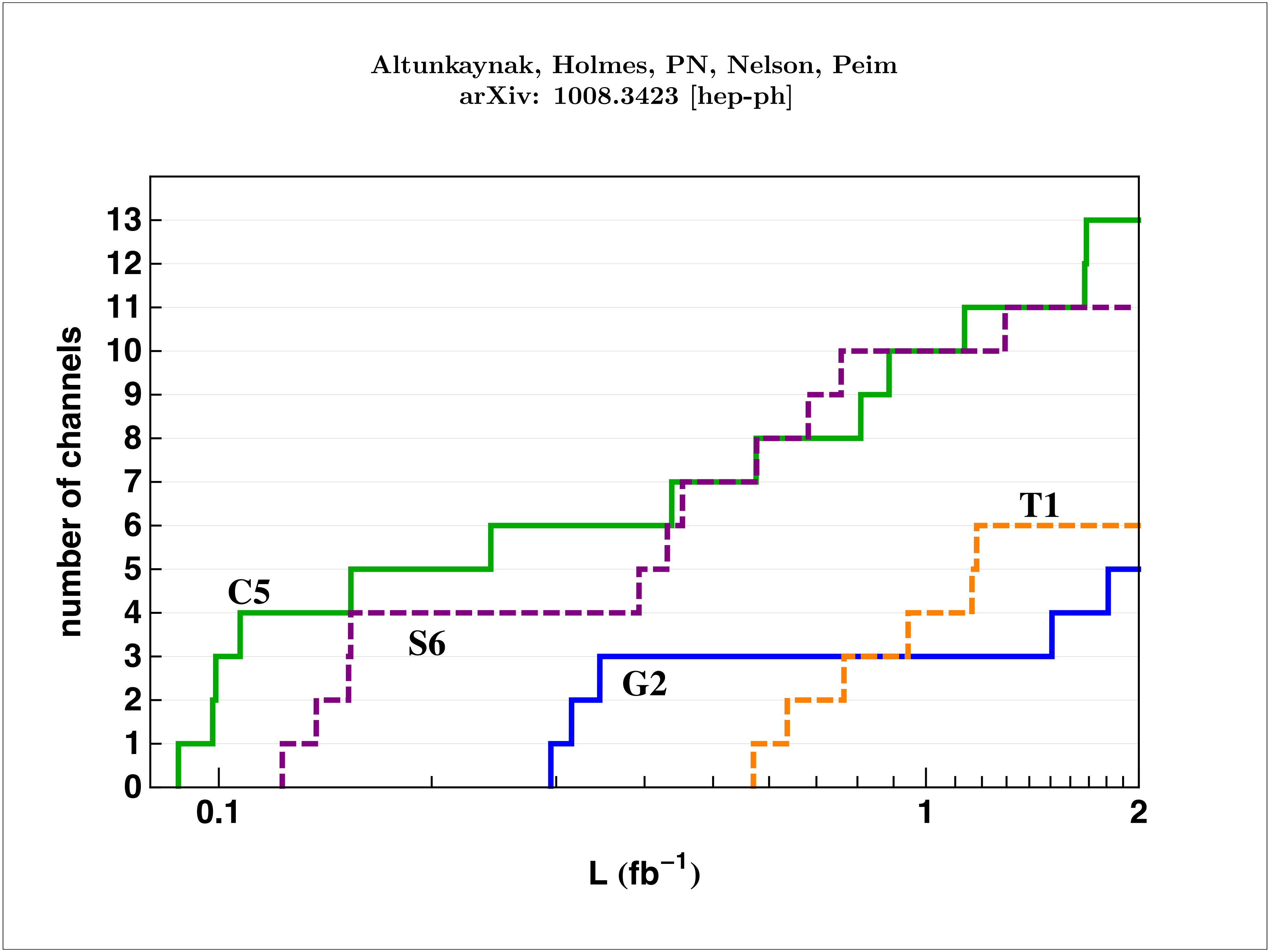

Altunkaynak, Holmes, PN, Nelson, Peim
arXiv: 1008.3423 [hep-ph]
number of channels
L (fb^{-1})
0.1
1
2
0
1
2
3
4
5
6
7
8
9
10
11
12
13
C5
S6
G2
T1

Altunkaynak, Holmes, PN, Nelson, Peim
arXiv: 1008.3423 [hep-ph]

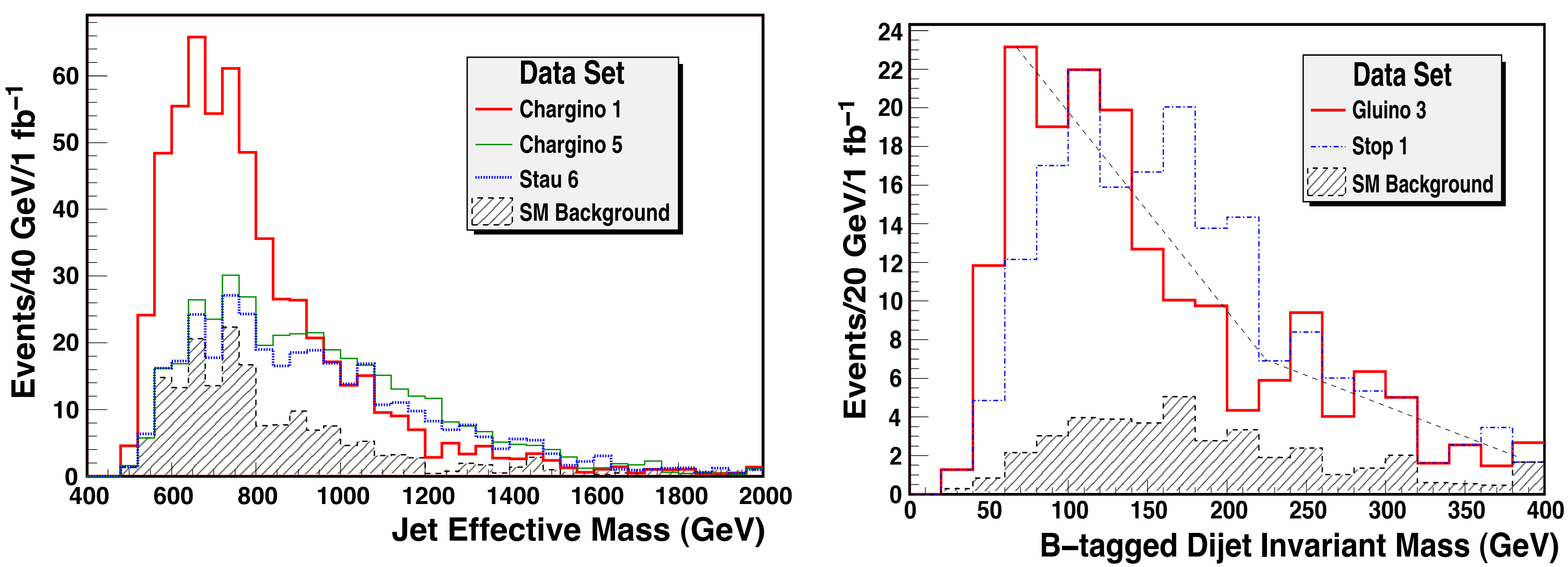

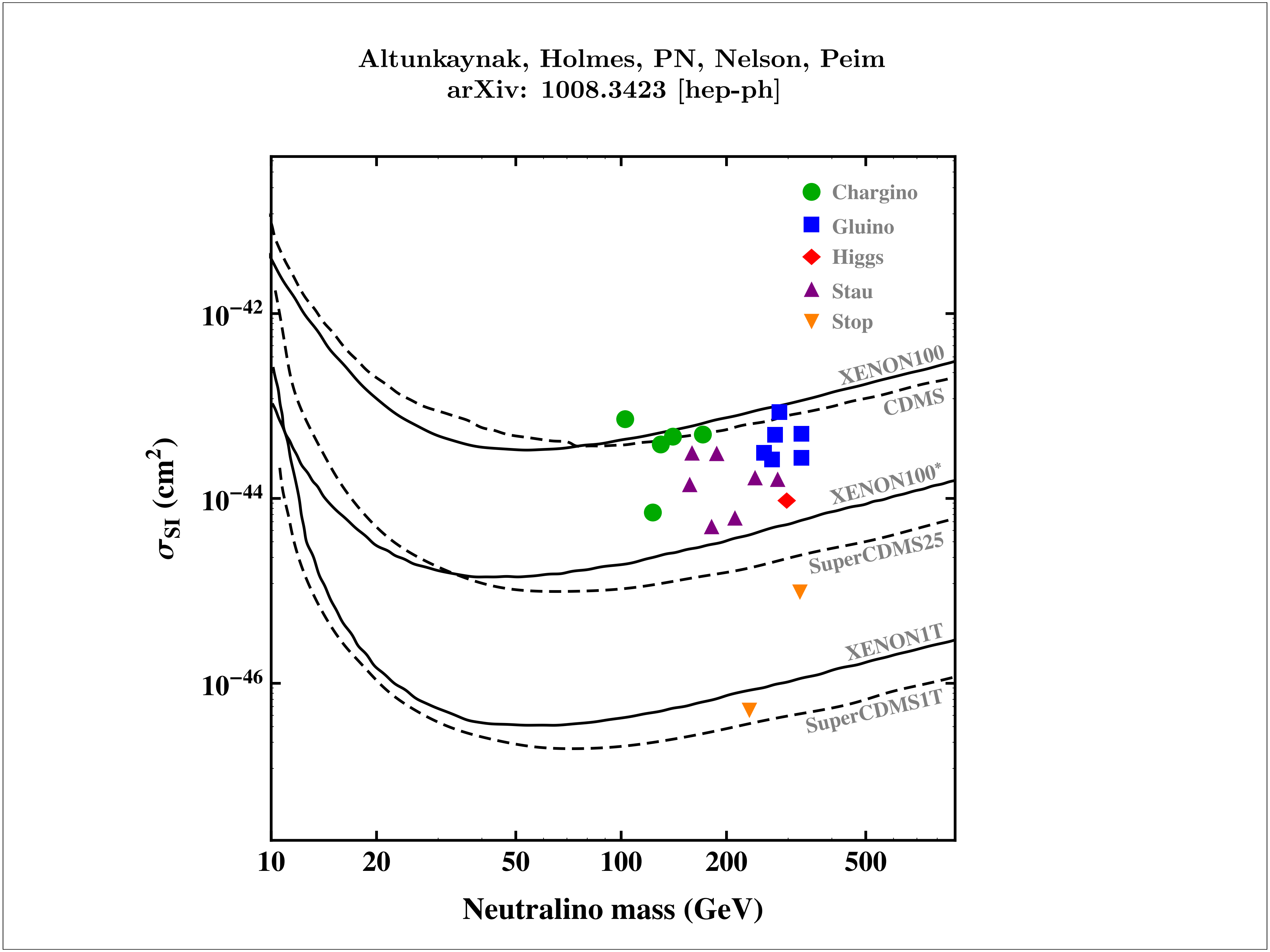

Altunkaynak, Holmes, PN, Nelson, Peim
arXiv: 1008.3423 [hep-ph]
Chargino
Gluino
Higgs
Stau
Stop
XENON100
CDMS
XENON100*
SuperCDMS25
XENON1T
SuperCDMS1T
10^{-42}
10^{-44}
10^{-46}
σ_{SI} (cm^2)
10
20
50
100
200
500
Neutralino mass (GeV)

Multicomponent dark matter

Feldman, Liu, PN, Peim, PRD81:095017,2010.

Dark matter may be constituted of more than one component

$$\Omega_{CDM} = \sum_i \Omega_{CDM i}.$$

We consider a $U(1)_X \times U(1)_C$ extension of SUGRA model where $U(1)_X$ is the hidden sector and $U(1)_C$ is the anomaly free combination $\mathcal{L}_e - \mathcal{L}_\mu$

$$\mathcal{L} = \mathcal{L}_{\text{MSSM}} + \mathcal{L}_{U(1)^2} + \Delta\mathcal{L}$$

$\mathcal{L}_{U(10^2}$ is the kinetic energy for the X and C multiplets and for $\mathcal{L}_{St}$ we assume the following form

$$\Delta\mathcal{L} = \int d^2\theta d^2\bar{\theta}[(M_1 C + M_2' X + S + \bar{S})^2 + (M_1' C + M_2 X + S' + \bar{S}')^2].$$

A Dirac fermion is placed in hidden sector [K. Cheung, T.C. Yuan; Feldman, Liu, PN]. The new particles in this model consist of

$$\text{spin } 0 : \rho, \rho', \phi, \phi'$$
$$\text{spin}\frac{1}{2} : \psi, \chi_5^0, \chi_6^0, \chi_7^0, \chi_8^0$$
$$\text{spin } 1 : Z', Z''.$$

Total relic density.

The total relic density is the sum of the Dirac and the Majorana components

$$(\Omega h^2)_{\mathrm{WMAP}} = (\Omega_\psi h^2) + (\Omega_\chi h^2) \sim \frac{C_\psi}{J_\psi} + \frac{C_\chi}{J_\chi}$$

$$C_\psi \simeq 2 \times \frac{1.07 \times 10^9 \mathrm{GeV}^{-1}}{\sqrt{g^*(\psi)} M_{\mathrm{Pl}}} C_\chi \simeq \times \frac{1.07 \times 10^9 \mathrm{GeV}^{-1}}{\sqrt{g^*(\chi)} M_{\mathrm{Pl}}}$$

$$J_\psi = \int_o^{x_f^\psi} < \sigma v >_{\psi\psi} dx, \quad J_\chi = \int_o^{x_f^\chi} < \sigma v >_{\chi\chi} dx$$

We assume the local density of dark matter proportional to the relic densities

$$\rho_{,\psi} / \rho_{,\chi} \sim (\Omega_\psi h^2)/(\Omega_\chi h^2)$$

To get the relic density one needs to solve coupled Boltzmann equations for the two component model

$$\frac{dn_\psi}{dt} = -3Hn_\psi - \frac{1}{2} < \sigma v >_{\psi\bar{\psi}} (n_\psi^2 - n_{\psi,eq}^2)$$
$$\frac{dn_\chi}{dt} = -3Hn_\chi - \frac{1}{2} < \sigma v >_{\chi\bar{\chi}} (n_\chi^2 - n_{\chi,eq}^2) + \frac{1}{2} < \sigma v >_{\psi\bar{\psi}} (n_\psi^2 - n_{\psi,eq}^2)$$

Two-component Dark Matter Model

Feldman, Liu, PN, Peim PRD 81:095017,2010, arXiv:1004.0649000

Positron flux

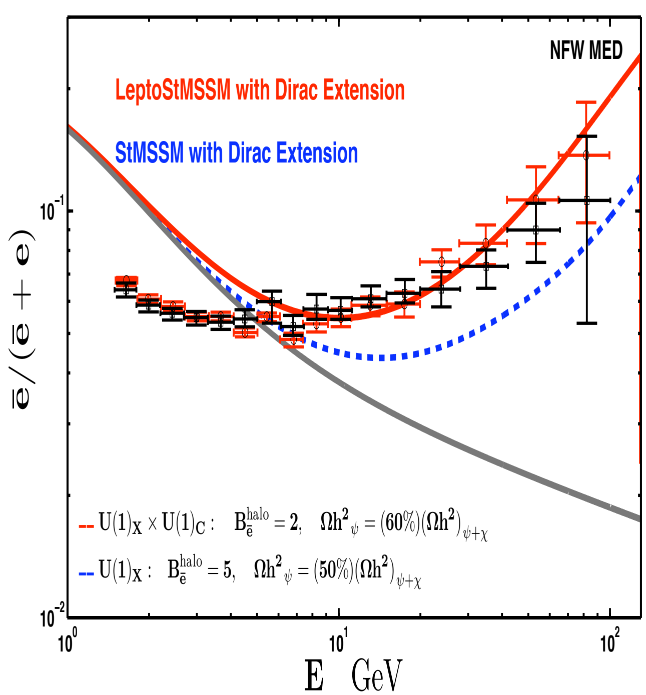

$\bar{p}$ flux

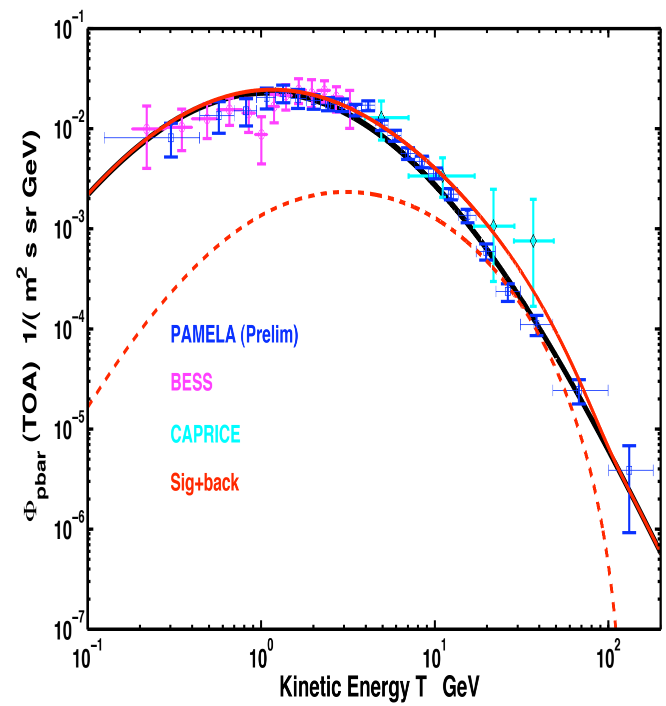

Two-component Dark Matter Model

Feldman, Liu, PN, Peim, PRD 81:095017,2010, arXiv:1004.0649000

Photon flux

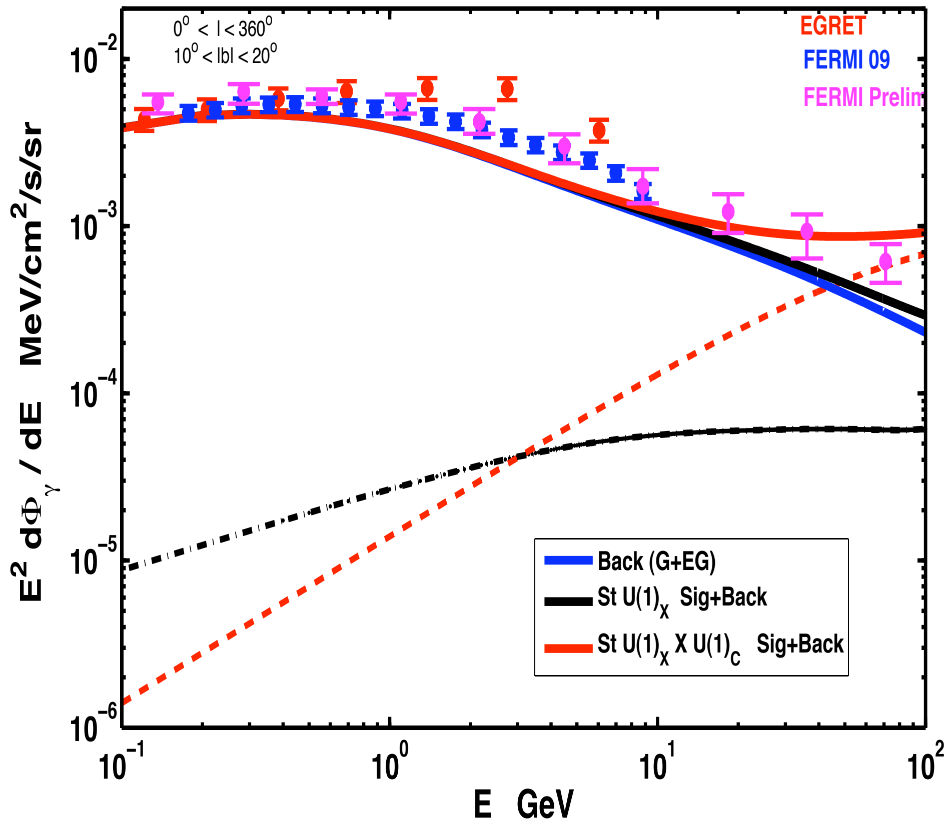

Two-component Dark Matter Model

Feldman, Liu, PN, Peim, PRD 81:095017,2010, arXiv:1004.0649000

σ_{SI}

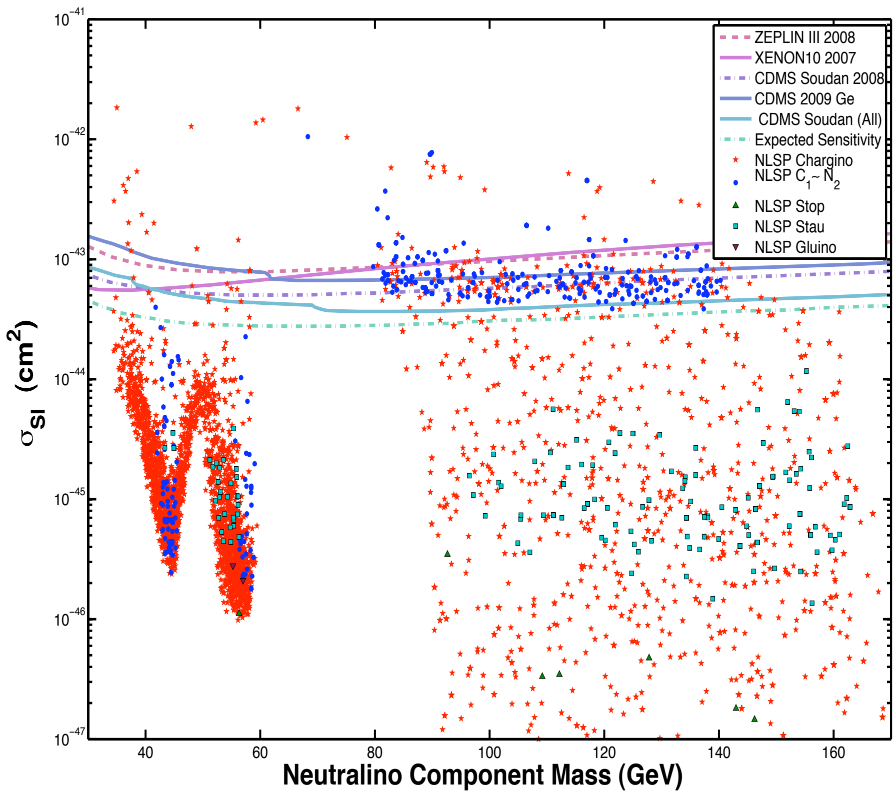

COGENT

Feldman, Liu, PN, PRD 81:117701,2010, arXiv: 1003.0437

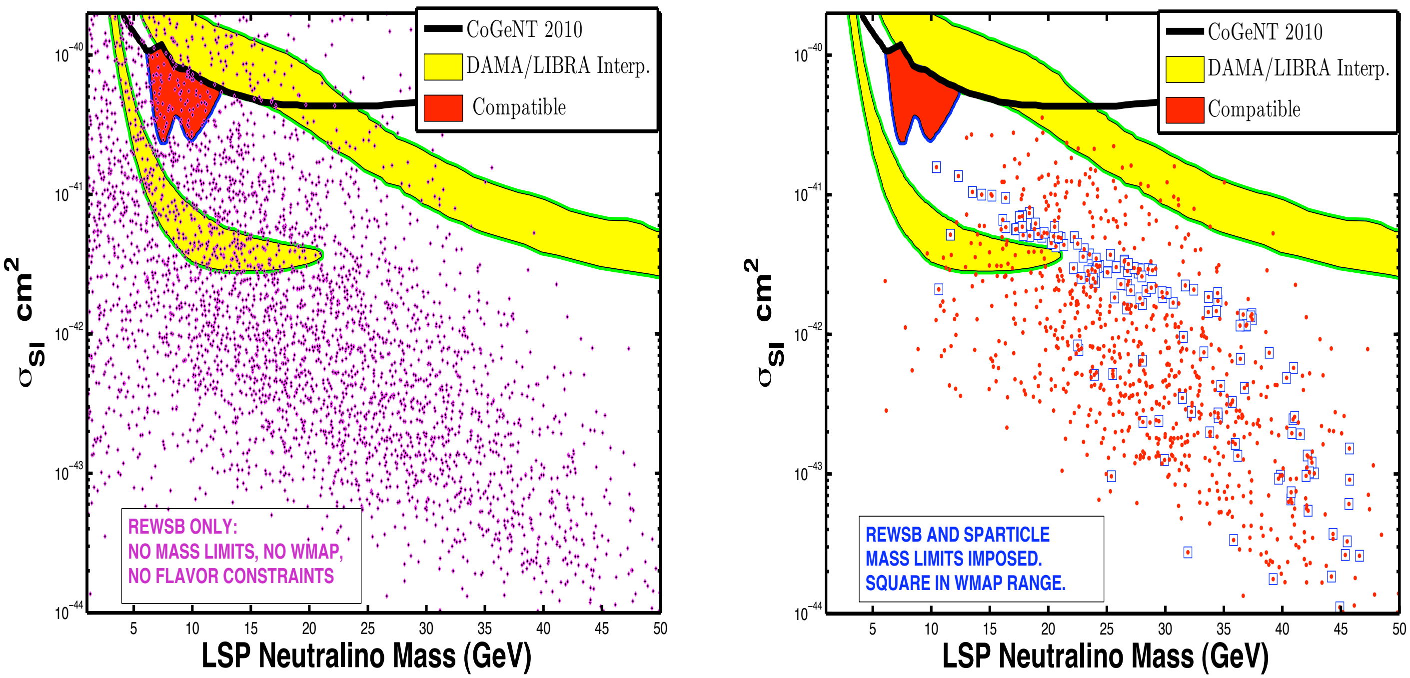

Difficult to get 10^{-40} cm^2 at $m_\chi = 10$ GeV with REWSB and experimental constraints.

Related works: Kuflick, Pierce, Zurek, Phys.Rev.D81:111701,2010,arXiv: 1003.0682, . . .

LHC data could decode the origin of dark matter in the early universe

Typically the relic density constraints are satisfied in four broad regions of the SUGRA parameter space

- Bulk region
- Pole region
- Coannihilation regions with coannihilations of neutralino with Wino, stau, stop, gluino $\cdots$
- Region with heavy scalars: Hyperbolic Branch/Focus Point region

  Chan, Chattopadhyay, PN; Feng, Matchev, Moroi; Baer, Tata, et.al. .

These regions can lead to distinguishable features at the LHC. As an illustration we contrast the signatures arising from the HB region vs the stau coannihilation region.

Hyperbolic Branch and stau coannihilation regions

- **On HB** the squarks are generally heavy and thus the gluinos are produced more profusely in this region than squarks. The gluinos have longer decay chains and thus missing P_T associated with this region is smaller

$$\tilde{g} \longrightarrow q\bar{q}\tilde{\chi}_i^0, \;\; q\bar{q}'\tilde{\chi}_j^{\pm}$$

  Also a larger multiplicity of quarks, specifically b quarks, produced in the HB region.

- **In the Stau Co-annihilation** region some of the squarks are relatively light and they are more profusely produced than gluinos. The squarks have shorter decay chains and thus missing P_T associated with this region is larger

$$\tilde{q} \longrightarrow q\tilde{\chi}_i^0, \; q'\tilde{\chi}_j^{\pm}$$

OSSF Di-lepton

Feldman, Liu, PN: JHEP 0804:054,2008.

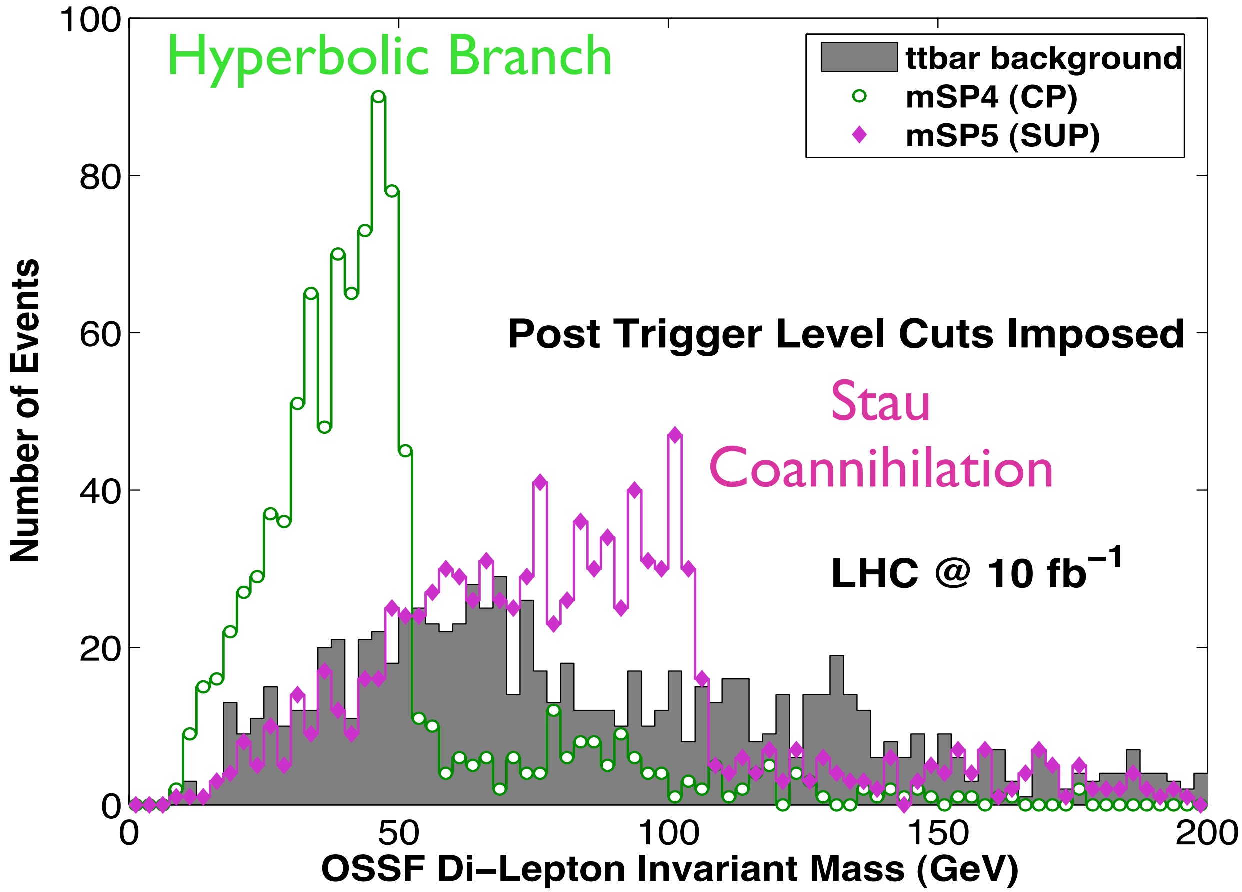

Feldman, Liu, PN: JHEP 0804:054,2008.

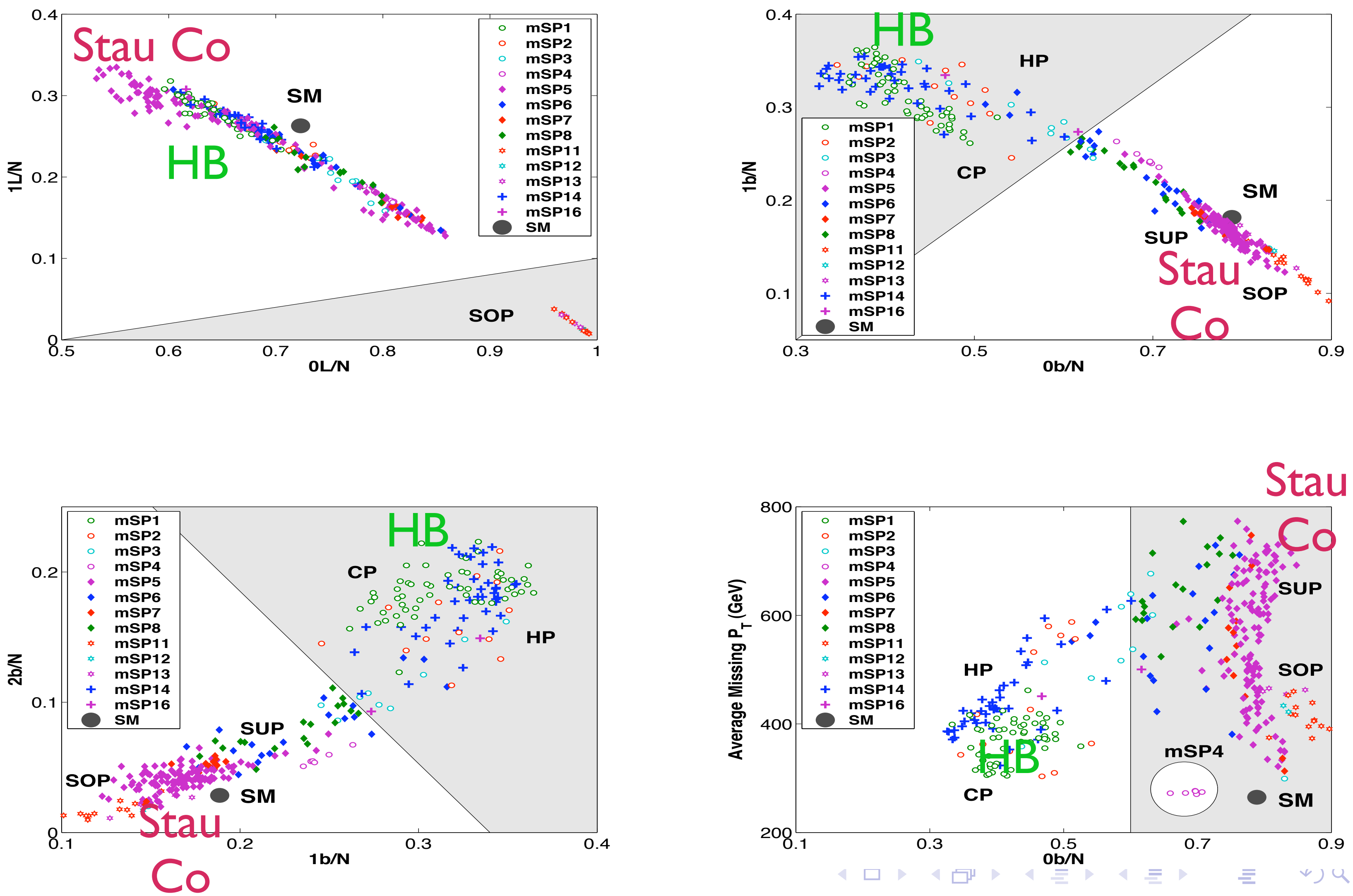

Conclusions

- An explanation of the various dark matter experiments in terms of partilcle physics phenomena suggests that the current pictures such as that of the standard SUSY models needs extension.
- We have discussed three possibilities all involving an extra hidden sector appended to the standard sugra picture. LHC data will be able to discriminate among these possibilities.
- Thus if the dark matter experimental results from PAMELA etc are real and further if one seeks particle physics explanation (as opposed to the astrophysical ones) then the hidden sector models are possible directions for further study.
- Low mass regions in the range of few hundred GeV can be explored with 1fb^{-1} of data at $\sqrt{s} = 7$ TeV and an early discovery of SUSY at the LHC is a distinct possibility.

Extra Slides

Altunkaynak, Holmes, PN, Nelson, Peim
arXiv: 1008.3423 [hep-ph]

A display of the Processes Analyzed and their standard model Backgrounds at $\sqrt{s} = 7$ TeV

SM Process	Cross Section (fb)	Number of Events	Luminosity (fb^{-1})
QCD $2, 3, 4$ jets (Cuts1)	2.0×10^{10}	74M	3.7×10^{-3}
QCD $2, 3, 4$ jets (Cuts2)	7.0×10^{8}	98M	0.14
QCD $2, 3, 4$ jets (Cuts3)	4.6×10^{7}	40M	0.88
QCD $2, 3, 4$ jets (Cuts4)	3.9×10^{5}	1.7M	4.4
$t\bar{t} + 0, 1, 2$ jets	1.6×10^{5}	4.8M	30
$b\bar{b} + 0, 1, 2$ jets	9.5×10^{7}	95M	1.0
$Z/\gamma\left(\rightarrow \ell\bar{\ell}, \nu\bar{\nu}\right) + 0, 1, 2, 3$ jets	6.2×10^{6}	6.2M	1.0
$W^{\pm}\left(\rightarrow \ell\nu\right) + 0, 1, 2, 3$ jets	1.9×10^{7}	21M	1.1
$Z/\gamma\left(\rightarrow \ell\bar{\ell}, \nu\bar{\nu}\right) + t\bar{t} + 0, 1, 2$ jets	56	1.0M	1.7×10^{4}
$Z/\gamma\left(\rightarrow \ell\bar{\ell}, \nu\bar{\nu}\right) + b\bar{b} + 0, 1, 2$ jets	2.8×10^{3}	0.1M	36
$W^{\pm}\left(\rightarrow \ell\nu\right) + b\bar{b} + 0, 1, 2$ jets	3.2×10^{3}	0.6M	1.8×10^{2}
$W^{\pm}\left(\rightarrow \ell\nu\right) + t\bar{t} + 0, 1, 2$ jets	70	4.6M	6.5×10^{4}
$W^{\pm}\left(\rightarrow \ell\nu\right) + t\bar{b}\,(\bar{t}b) + 0, 1, 2$ jets	2.4×10^{2}	2.1M	8.7×10^{3}
$t\bar{t}t\bar{t}$	0.5	0.09M	1.8×10^{5}
$t\bar{t}b\bar{b}$	1.2×10^{2}	0.32M	2.7×10^{3}
$b\bar{b}b\bar{b}$	2.2×10^{4}	0.22M	1.0
$W^{\pm}\left(\rightarrow \ell\nu\right) + W^{\pm}\left(\rightarrow \ell\nu\right)$	2.0×10^{3}	0.05M	25
$W^{\pm}\left(\rightarrow \ell\nu\right) + Z\left(\rightarrow\ all\right)$	1.1×10^{3}	1.3M	1.1×10^{3}
$Z\left(\rightarrow\ all\right) + Z\left(\rightarrow\ all\right)$	7.3×10^{2}	2.6M	3.6×10^{3}
$\gamma + 1, 2, 3$ jets	1.5×10^{7}	16M	1.1

TABLE I: An exhibition of the standard model backgrounds computed in this work at $\sqrt{s} = 7$ TeV. All processes were generated using MadGraph 4.4 [10]. Our notation here is that $\ell = e, \mu, \tau$ and $all = \ell, \nu, jets$. Cuts1-Cuts4 indicated in the table are defined in Eq. (1). In the background analysis we eliminate double counting between the process $W^{\pm} + t\bar{b}\,(\bar{t}b)$ and $t\bar{t}$ by subtracting out double resonant diagrams of $t\bar{t}$ when calculating $W^{\pm} + t\bar{b}\,(\bar{t}b)$.[3]

Altunkaynak, Holmes, PN, Nelson, Peim
arXiv: 1008.3423 [hep-ph]

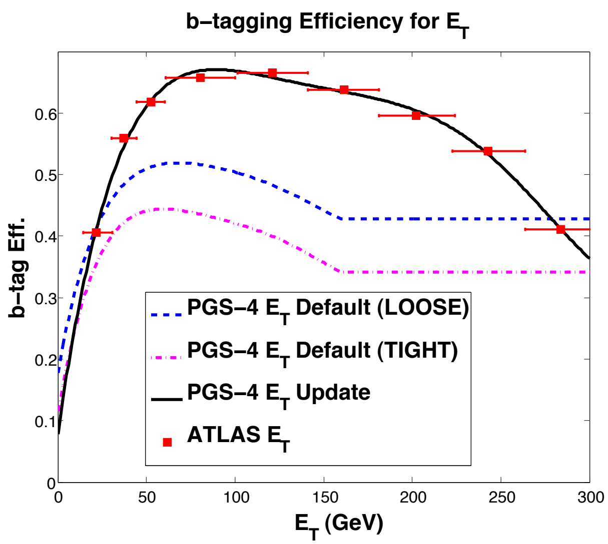

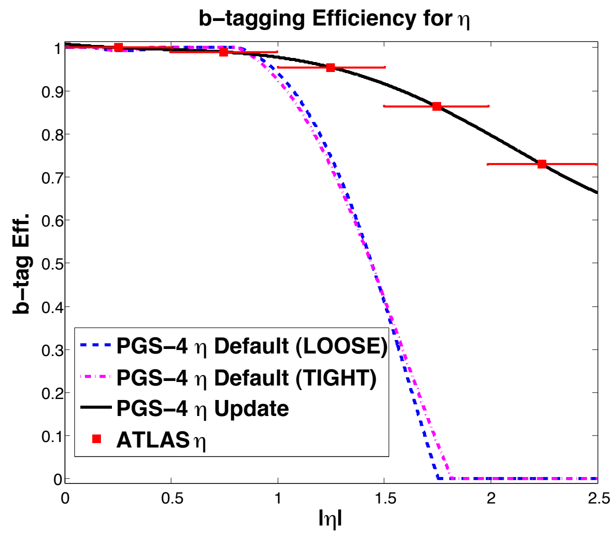

Altunkaynak, Holmes, PN, Nelson, Peim
arXiv: 1008.3423 [hep-ph]

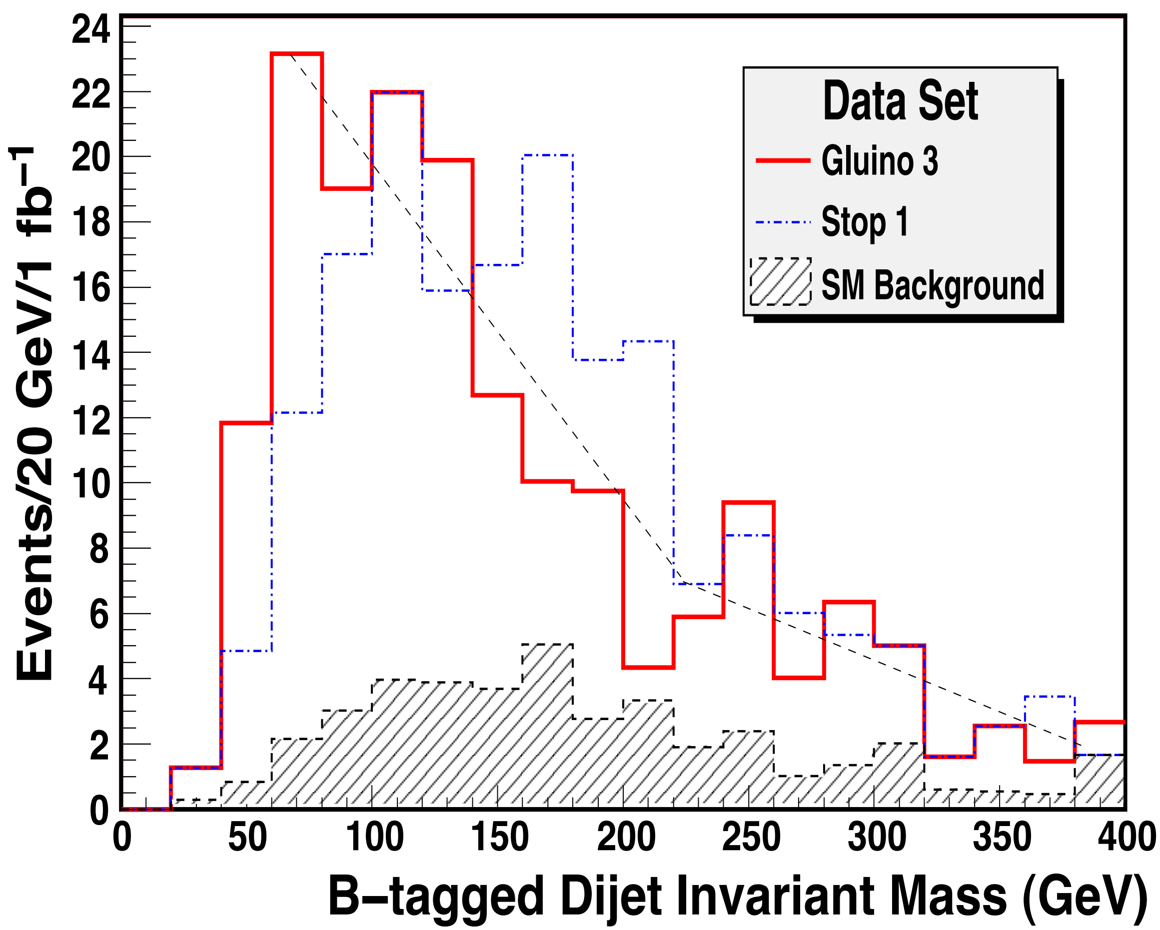

Altunkaynak, Holmes, PN, Nelson, Peim
arXiv: 1008.3423 [hep-ph]

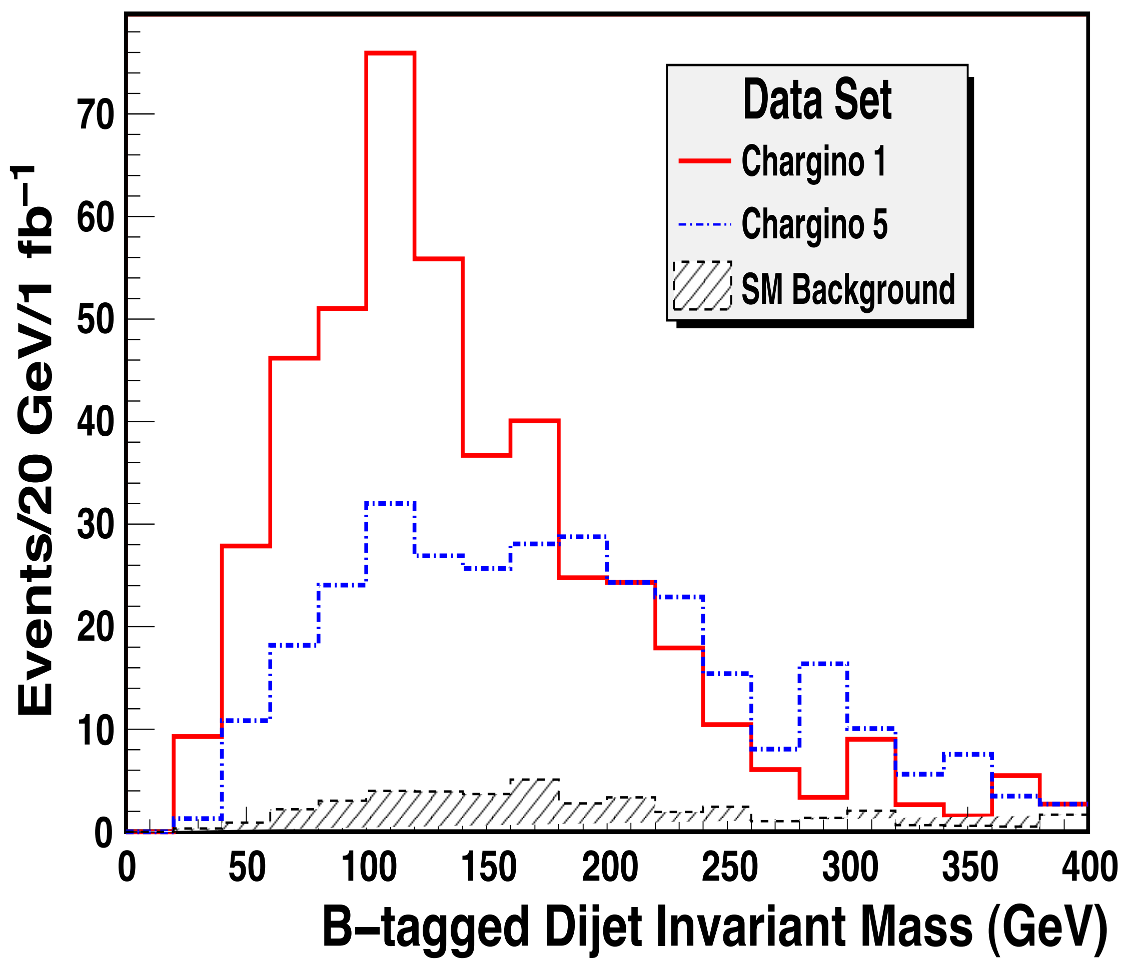

Altunkaynak, Holmes, PN, Nelson, Peim
arXiv: 1008.3423 [hep-ph]